PLOS PATHOGENS

RESEARCH ARTICLE

The inclusion membrane protein IncS is critical for initiation of the *Chlamydia* intracellular developmental cycle

María Eugenia Cortina[1], R. Clayton Bishop[1], Brittany A. DeVasure[1], Isabelle Coppens[2], Isabelle Derré[1]*

1 Department of Microbiology, Immunology, and Cancer Biology, University of Virginia School of Medicine, Charlottesville, Virginia, United States of America, **2** Department of Molecular Microbiology and Immunology, Johns Hopkins School of Public Health, Baltimore, Maryland, United States of America

* id8m@virginia.edu

Citation: Cortina ME, Bishop RC, DeVasure BA, Coppens I, Derré I (2022) The inclusion membrane protein IncS is critical for initiation of the *Chlamydia* intracellular developmental cycle. PLoS Pathog 18(9): e1010818. https://doi.org/10.1371/journal.ppat.1010818

Editor: Richard D. Hayward, University of Cambridge, UNITED KINGDOM

Received: March 6, 2022

Accepted: August 22, 2022

Published: September 9, 2022

Data Availability Statement: All relevant data are within the manuscript and its Supporting Information files.

Funding: This work was supported by funding from the National Institute of Allergy and Infectious Diseases of the United States of America: research grants AI101441, AI162758 and AI166237 to ID and research grants AI060767 and AI166921 to IC. The funders had no role in study design, data collection and analysis, decision to publish, or preparation of the manuscript.

Abstract

All *Chlamydia* species are obligate intracellular bacteria that undergo a unique biphasic developmental cycle strictly in the lumen of a membrane bound compartment, the inclusion. *Chlamydia* specific Type III secreted effectors, known as inclusion membrane proteins (Inc), are embedded into the inclusion membrane. Progression through the developmental cycle, in particular early events of conversion from infectious (EB) to replicative (RB) bacteria, is important for intracellular replication, but poorly understood. Here, we identified the inclusion membrane protein IncS as a critical factor for *Chlamydia* development. We show that a *C. trachomatis* conditional mutant is impaired in transition from EB to RB in human cells, and *C. muridarum* mutant bacteria fail to develop in a mouse model of *Chlamydia* infection. Thus, IncS represents a promising target for therapeutic intervention of the leading cause of sexually transmitted infections of bacterial origin.

Author summary

The identification and characterization of bacterial factors that are essential, or highly important, to the intracellular life style of obligate intracellular bacterial pathogens, for which limited genetic tools exist, present unique challenges. Here, we offer a blueprint to generate conditional mutants in *Chlamydia trachomatis* and *Chlamydia muridarum*, by combining existing genetic tools for *Chlamydia*, including an inducible promoter that is responsive in a murine model of *Chlamydia* infection. As a proof of concept, we present a conditional mutant in a *Chlamydia* inclusion membrane protein and show that it is impaired in the early stages of the developmental cycle. Our study constitutes a major methodological advance to the study of *Chlamydia* and furthers our understanding of the bacterial factors contributing to progression through the developmental cycle.

Competing interests: The authors have declared that no competing interests exist.

Introduction

C. trachomatis is the leading cause of bacterial sexually transmitted diseases. 1.7 million cases are reported in the United States annually, and there are an estimated 131 million new cases each year worldwide [1, 2]. Infections are often asymptomatic, especially in women, which increases the risks of transmission to sex partners. In addition, if left untreated, cervical infections ascend to the upper genital tract resulting in tissue inflammation leading to pelvic inflammatory disease, ectopic pregnancy and infertility [3]. Vaccines are not available [4, 5], and because of short-lived protective immunity from infection, reinfection rates are high and contribute to the aggravation of the long-term sequelae associated with infection.

All *Chlamydia* species are obligate intracellular bacteria that replicate exclusively in epithelial cells within a membrane-bound compartment, termed the inclusion, and via a unique biphasic developmental cycle [6]. The first 8 hours are especially critical in establishing a replicative niche because invaded, infectious, morphologically small, but non-replicative elementary body (EB) must transition to replicative, morphologically larger, albeit non-infectious, reticulate body (RB). Concomitantly, the nascent inclusions traffic along microtubules to the microtubule organizing center (MTOC) [7]. Bacterial transcription and translation are both required during the early events of the developmental cycle [7]; however, the specific mechanism(s) by which EB transition to RB is unclear.

Inclusion membrane proteins (Inc) are *Chlamydia*-specific Type III secretion effector proteins that are embedded into the inclusion membrane and proposed to facilitate inclusion maturation and inclusion membrane stability [8, 9]. *Chlamydia* encodes 50–100 putative Inc proteins, some, but not all, are conserved among species [10–13]. A comprehensive list of Inc-host protein interactions was identified, and in part validated [9, 14]. Nevertheless, the specific functions of many Inc proteins remain elusive, due much to a lag in *Chlamydia* genetics [15]. Recent progress led to the identification of a few *C. trachomatis inc* mutants with *in vitro* and/or *in vivo* defects [12, 16–18]. However, none of them have been implicated in the early stages of the developmental cycle. Additionally, in light of the obligate intracellular lifestyle of the pathogen, the overall viability of the above-mentioned *C. trachomatis* mutants and the fact that they were identified in the first place, indicate that the corresponding Inc proteins are not essential.

Essential virulence factors, preferably common to all *Chlamydia* species, would be ideal drug targets to limit the spread of the bacteria. They remain unknown, and their identification is challenging. Without the option of cultivating the bacteria in axenic medium, *Chlamydia* mutants with severe intracellular developmental defects cannot be propagated and therefore would be missed using current targeted or unbiased genetic approaches. Here, through the use of *C. trachomatis* and *C. muridarum* conditional mutants, we report a conserved Inc protein that plays a critical role in initiation the *Chlamydia* developmental cycle *in vitro* and *in vivo*.

Results

Generation of a *C. trachomatis incS* conditional mutant overcomes IncS requirement in cell culture

To investigate the role of the *C. trachomatis* Inc protein CTL0402, we sought to generate a *ctl0402* mutant using TargeTron or FRAEM (fluorescence reported allelic exchange mutagenesis) [19, 20]. After several unsuccessful attempts, we hypothesized that *ctl0402* may be required for proper bacterial development in cell culture. CTL0402 was renamed $IncS_{Ct}$, and we developed a 4-step strategy to generate a $\Delta incS_{Ct}$ conditional FRAEM mutant (Fig 1A). *C. trachomatis* wild-type was first transformed with the pSU-ΔincS plasmid which encodes the *aadA-gfp* selection cassette surrounded by chlamydial DNA corresponding to ~3 kb of genomic

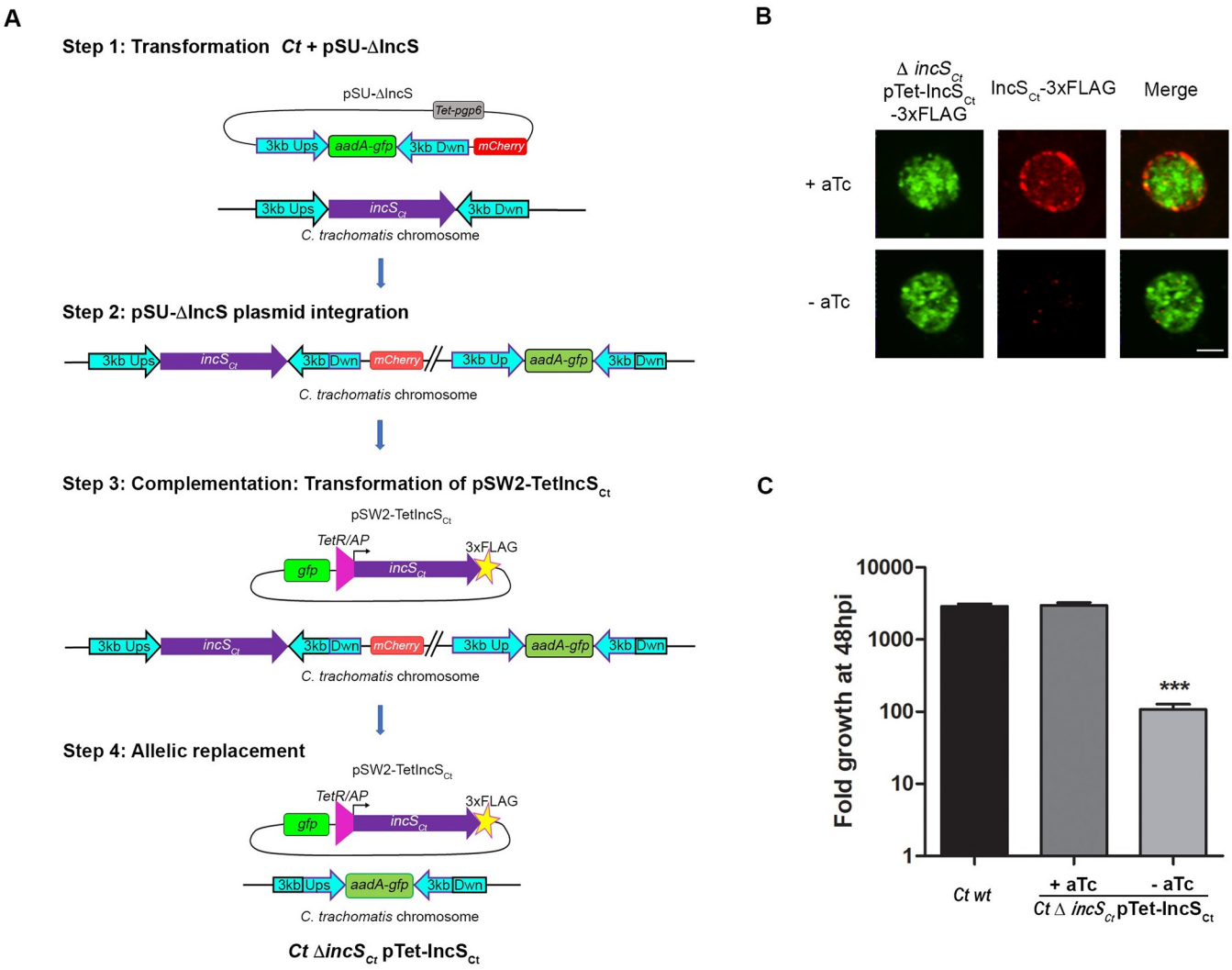

Fig 1. A *Chlamydia trachomatis incS* conditional mutant displays a severe growth defect in cell culture. (A) Schematic representation of the modified 4-step FRAEM strategy used to generate a *C. trachomatis incS* conditional mutant (*Ct ΔincS*$_{Ct}$ pTet-IncS$_{Ct}$). Step1: Transformation of wild-type *C. trachomatis*, containing an intact chromosomal *incS*$_{Ct}$ ORF (purple), with pSU-Δ*incS* harboring ~3kb homology sequence upstream and downstream of the *incS* ORF (3kb Ups and 3kb Dwn, respectively, cyan) flanking the *aadA-gfp* selection cassette (green), mCherry (red), and the plasmid maintenance ORF *pgp6* under the control of the aTc inducible promoter (gray). Step 2: Integration of pSU-Δ*incS* in the *C. trachomatis* chromosome upstream or downstream (shown here) of the *incS* ORF, via a single recombination event, resulting in a strain displaying dim green and red fluorescence. Step 3: Transformation of the strain resulting from step 2 with pSW2-Tet-IncS$_{Ct}$, a complementation plasmid encoding GFP (green) and a 3x-FLAG tagged (yellow star) allele of IncS$_{Ct}$ (purple) under the control of the aTc inducible promoter (TetR/AP, pink triangle). Step 4: Expression of IncS from the complementation plasmid, allows for allelic replacement of the chromosomal *incS* ORF with the *aadA-gfp* cassette and loss of mCherry, via a second event of recombination within the 3 kb upstream sequence. (B) Three-dimensional confocal micrographs of HeLa cells infected for 24h with the *C. trachomatis ΔincS*$_{Ct}$ conditional mutant expressing GFP (*ΔincS*$_{Ct}$ pTet-IncS$_{Ct}$-3xFLAG, left panels, green) in the presence (+aTc, top panels) or the absence (-aTc, bottom panels) of aTc and stained with anti-FLAG antibody (IncS$_{Ct}$-3xFLAG, middle panels, red). The merge is shown on the right. Scale bar: 5μm. (C) Fold growth of wild-type *C. trachomatis* (*Ct wt*) and the *C. trachomatis ΔincS*$_{Ct}$ conditional mutant (Δ*incS*$_{Ct}$ pTet-IncS$_{Ct}$) in HeLa cells at 48h pi compared to 0h pi in the presence (+aTc) or absence (-aTc) of aTc. Data are mean ± SEM, three combined experiments, One-way ANOVA, Tukey's Multiple Comparison Test, *** P<0.001 (-aTc vs + aTc or wt).

https://doi.org/10.1371/journal.ppat.1010818.g001

sequence flanking the *incS*$_{Ct}$ ORF, mCherry under the control of a constitutive promoter, and the *Chlamydia* plasmid maintenance ORF *pgp6* under the control of the anhydrotetracycline (aTc) inducible promoter (Fig 1A Step 1). GFP- and mCherry-positive transformants were selected in the presence of 500 μg/ml of Spectinomycin (Spec) and 50 ng/ml of aTc. Chromosomal integration of pSUΔincS via a single event of recombination within a 3kb region upstream, or downstream, of the *incS*$_{Ct}$ ORF, indicated by dim green and red fluorescence,

was accomplished by cultivating the transformants in the absence of aTc for multiple passages at low MOI (~0.2) (Fig 1A Step 2). The resulting strain was transformed with pSW2-TetIncS$_{Ct}$, a complementation plasmid carrying a 3xFLAG tagged allele of IncS$_{Ct}$ under the control of the aTc inducible promoter, in the presence of 0.5 ng/ml aTc, 500 μg/ml Spec and 1U Penicillin G (Fig 1A Step 3). The aTc concentration was empirically determined based on the detection of low levels of IncS$_{Ct}$-3xFLAG at the inclusion membrane, when expressed in wild-type *C. trachomatis* (not shown). After several passages at a low MOI in the presence of aTc, Spec and Penicillin G, a second event of recombination occurred in some bacteria, leading to the allelic replacement of the *incS$_{Ct}$* ORF with an *aadA-gfp* cassette and the loss of mCherry expression (Fig 1A Step 4). Once the population reached 50% of GFP-positive and mCherry-negative inclusions, the bacteria were plaque purified. The resulting *C. trachomatis* strain (*Ct ΔincS$_{Ct}$* pTet-IncS$_{Ct}$) is referred to as the *ΔincS$_{Ct}$* conditional mutant. Three independent clones were amplified, validated as follow, and shown to display the same phenotype. Allelic exchange was confirmed by PCR (S1 Fig). The conditional expression and inclusion localization of IncS$_{Ct}$ was validated by immunofluorescence (Fig 1B). To determine if the lack of IncS affected the production of infectious progeny, cells were infected with the *ΔincS$_{Ct}$* conditional mutant in the presence or absence of aTc for 48h pi, and recovered infectious bacteria were enumerated on a fresh monolayer of cells (Fig 1C). Wild-type *C. trachomatis* expressing mCherry constitutively was used as a positive control. In the absence of aTc, the *ΔincS$_{Ct}$* conditional mutant presented a 1.5-log reduction in the number of infectious progenies, compared to the complemented strain, which yielded similar number of infectious progenies as the wild-type strain. Thus, as predicted by our failed attempts to generate a *C. trachomatis incS* mutant, the lack of IncS leads to a severe growth defect, and IncS requirement in cell culture can be bypassed by generating a conditional mutant.

A *C. trachomatis incS* mutant fails to initiate the developmental cycle

We next sought to investigate the nature of the growth defect of the *ΔincS$_{Ct}$* mutant by inducing or terminating complementation at different times post infection (Fig 2). Cells were infected with the *C. trachomatis ΔincS$_{Ct}$* conditional mutant at an MOI of 1 in the absence (Fig 2A) or the presence of aTc (Fig 2B). Infections were synchronized by centrifugation and extensive washes of the monolayers. At 2, 4, 6 or 8h pi, the medium was replaced with 0.5ng/ml aTc (Fig 2A) or medium without aTc (Fig 2B), and the number of infected cells was quantified at 28h pi. The substantial decrease in infectious progeny observed at 48h pi (Fig 1C) correlated with a drastic reduction in the number of infected cells harboring an inclusion at 28h pi (Fig 2A -aTc). Additionally, complementation induction (Fig 2A) or termination (Fig 2B) at different times post infection revealed that *incS* expression was required during the early stages of the developmental cycle, more specifically the first 6-8h, a time at which transition from EB to RB occurs.

To further investigate the intracellular localization and morphology of the *ΔincS$_{Ct}$* mutant bacteria during the early stages of the developmental cycle, cells were infected with the *C. trachomatis ΔincS$_{Ct}$* conditional mutant at an MOI of 10 with or without aTc, or with aTc added beginning at 4h pi. Infections were synchronized as described above. Infected cells, stained with a DNA dye, were analyzed by confocal microscopy at 12h pi. EB- and RB-like bacteria were identified based on the size of their respective DNA signal (small and large, respectively) and the number of total and large RB-like intracellular bacteria that clustered at the MTOC were determined (Fig 2C–2E). Regardless of complementation, by 12h pi, a similar number of intracellular bacteria clustered at the MTOC (Fig 2C and 2D). However, the number of bacteria with an RB morphology was significantly reduced in the absence of complementation (Fig

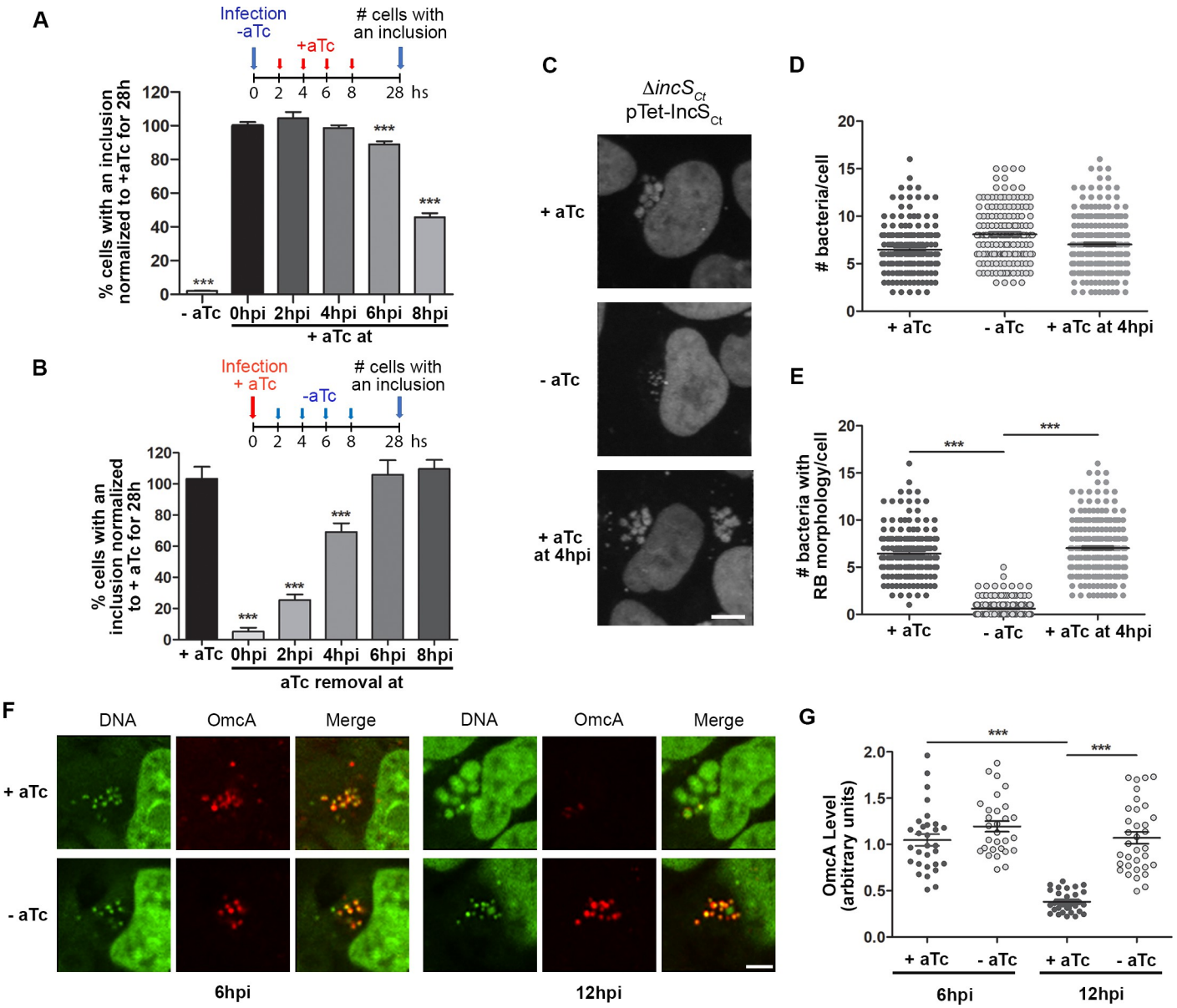

Fig 2. Early developmental defect of a *Chlamydia trachomatis incS* conditional mutant. (A-B) Percentage of cells displaying an inclusion at 28h pi after infection with *C. trachomatis* $\Delta incS_{Ct}$ conditional mutant. Infections were initiated in the absence (A) or presence (B) of aTc, and aTc was added (A) or removed (B) at the indicated time. Infections carried out in the absence (A, -aTc) or presence (B, +aTc) served as controls. Data are mean ± SEM normalized to 0h (A) or +aTc (B), one representative experiment of n = 3, One-Way ANOVA, Dunnett's Multiple Comparison, *** P<0.001. (C) Three-dimensional confocal micrographs of HeLa cells infected with *C. trachomatis* $\Delta incS_{Ct}$ conditional mutant at an MOI of 10 for 12h in the presence (+aTc) or absence (-aTc) of aTc, or in absence of aTc for the first 4h only (+aTc 4h pi) and stained the DNA dye 7AAD-red. Scale bar: 5μm. (D-E) Quantification of number of bacteria per cell (D) and the number of bacteria with an RB morphology (E), as shown in (C). Each data point represents an infected cell, the mean ± SEM of one representative experiment of n = 3 is shown, One-Way ANOVA, Tukey's Multiple Comparison, *** P<0.001. (F) Representative single plane confocal micrographs of HeLa cells infected with *C. trachomatis* $\Delta incS_{Ct}$ conditional mutant for 6h (left panels) or 12h (right panels) in the presence (+aTc) or absence (-aTc) of aTc and stained with the EB-specific marker OmcA (red) and the DNA dye SytoxGreen (green). Scale bar: 5μm. (G) Quantification of the levels of OmcA associated with perinuclear bacteria as shown in (F). Each data point represents an infected cell, the mean ± SEM of one representative experiment of n = 3 is shown, One-Way ANOVA, Tukey's Multiple Comparison, *** P<0.001.

https://doi.org/10.1371/journal.ppat.1010818.g002

2C and 2E). This phenotype was reverted by complementation at 4h pi. These results suggested that, in cell culture, the *C. trachomatis* $\Delta incS_{Ct}$ mutant may be compromised in transitioning from EB to RB.

To more directly assess if the *C. trachomatis* $\Delta incS_{Ct}$ mutant fails to transition from EB to RB, we performed transmission electron microscopy (TEM) for morphological analysis of the bacteria at 12h pi (S2 Fig). TEM allows to distinguish between EB and RB based on differences in size and electron (e)-density, with EB appearing as small e-dense (black) cocci of ~250 nm in diameter and RB as less e-dense (grey) cocci of ~1 μm in diameter, respectively. Additionally, bacteria transitioning from EB to RB form an Intermediate Body (IB) appearing as small grey cocci of ~500 nm in diameter with a darker center corresponding to condensed chromosomal material. TEM section of inclusions harboring the complemented $\Delta incS_{Ct}$ mutant all contained dividing RBs (S2 Fig, +aTc 12hpi), while EB- or IB-containing inclusions were not observed under this condition. In comparison, while some RB-containing inclusions were observed in cells infected with the $\Delta incS_{Ct}$ mutant, a notable number of inclusions contained bacteria with a size and morphology reminiscent of IBs (S2 Fig, -aTc 12hpi). We estimated that approximately one third of the $\Delta incS_{Ct}$ mutant inclusions contained RBs, one third contained EBs, and one third contained IBs (not shown).

As a complementary approach, we used antibodies against the EB-specific OmcA protein [21] to perform quantitative confocal analysis of the presence of EBs in cells infected with the *C. trachomatis* $\Delta incS_{Ct}$ conditional mutant with or without aTc (Fig 2F and 2G). Our quantification method is detailed in S3 Fig. At 6h pi, complemented and $\Delta incS_{Ct}$ mutant bacteria clustered at the MTOC displayed equivalent levels of OmcA. However, at 12h pi, the complemented $\Delta incS_{Ct}$ mutant bacteria were OmcA-negative, whereas the $\Delta incS_{Ct}$ mutant bacteria remained OmcA-positive, further supporting that by 12h pi $\Delta incS_{Ct}$ mutant bacteria retained EB-like characteristics.

Collectively, these results indicate that, in cell culture, the severe growth defect of the *C. trachomatis* $\Delta incS_{Ct}$ mutant occurs early in the developmental cycle, most likely due to failure of the bacteria to transition from EB to RB.

IncS requirement to establish a productive infection in cell culture is conserved in *C. muridarum*

C. trachomatis does not establish a productive infection in mice and is rapidly cleared from the murine genital tract [22]; however, upon infection with the murine-adapted species *C. muridarum*, mice do recapitulate hallmarks of *Chlamydia* infections observed in women [23]. Therefore, to investigate the role of IncS *in vivo*, we generated a *C. muridarum* $incS_{Cm}$ (*tc0424*) conditional mutant. FRAEM is not available for *C. muridarum*, therefore we developed a 3-step TargeTron-based approach (Fig 3A). *C. muridarum* wild-type was first transformed with pNigg-TetIncS$_{Ct}$ (Fig 3A Step 1). Following 3 passages in the presence of 500 μg/ml Spec, transformants were plaque purified and transformed with pDFTT3-IncS$_{Cm}$ (Fig 3A Step 2). The chromosomal integration of the intron/β-lactamase (*bla*) resistance cassette at nucleotide position 412 of the *incS* ORF was selected for in the presence of 1 ng/ml aTc, 500 μg/ml of Spec and 1U PenG. The aTc concentration was empirically determined based on the detection of low levels of IncS$_{Cm}$-3xFLAG at the inclusion membrane, when expressed in wild-type *C. muridarum* (not shown). The resulting *C. muridarum* strain (*Cm* $incS_{Cm}$::*bla* pTet-IncS$_{Ct}$) is referred to as the $incS_{Cm}$::*bla* conditional mutant. Three independent plaque purified clones were amplified, validated as follow, and shown to display the same phenotype. Intron integration was confirmed by PCR and sequencing (S4 Fig). The conditional expression and inclusion localization of IncS$_{Ct}$ was validated by immunofluorescence (Fig 3B). To determine if inactivation of $incS_{Cm}$ led to a growth defect in *C. muridarum*, cells were infected with the $incS_{Cm}$::*bla* conditional mutant in the presence or absence of aTc, and the production of infectious progeny was assessed at 39h pi (Fig 3C). Wild-type *C. muridarum* expressing mCherry constitutively was used as a positive control. In the

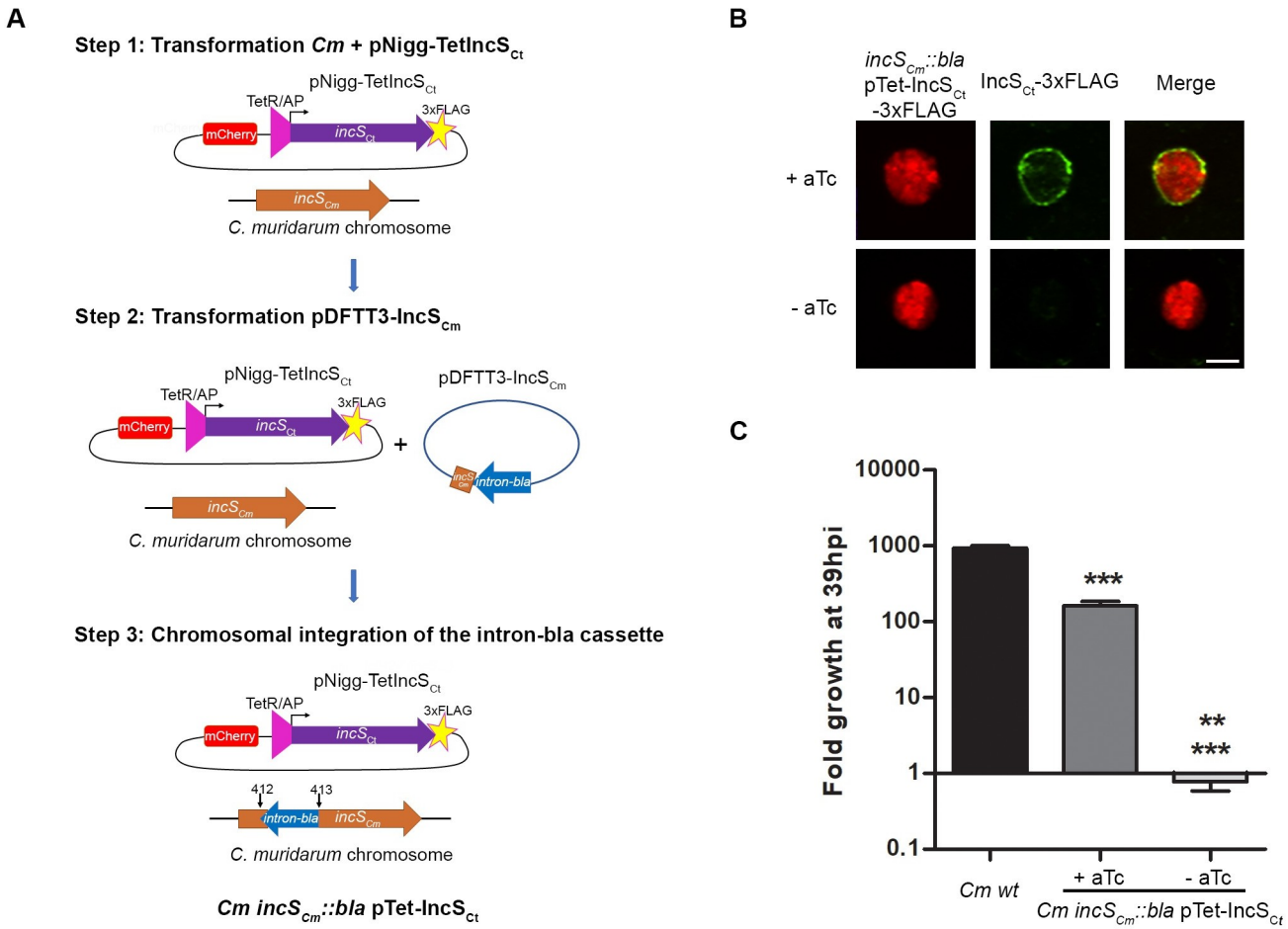

Fig 3. *Chlamydia muridarum incS* conditional mutant displays a severe growth defect in cell culture. (A) Schematic representation of the modified 3-step Targetron strategy used to generate a *C. muridarum incS*$_{Cm}$ (*tc0424*) conditional mutant (*Cm incS*$_{Cm}$*::bla* pTet-IncS$_{Ct}$). Step1: Transformation of wild-type *C. muridarum*, containing an intact chromosomal *incS*$_{Cm}$ ORF (brown), with pNigg-Tet-IncS$_{Ct}$, a complementation plasmid encoding mCherry (red) and a 3x-FLAG tagged (yellow star) allele of IncS$_{Ct}$ (purple) under the control of aTc inducible promoter (TetR/AP, pink triangle). Step 2: Transformation of the strain resulting from step 1 with pDFTT3-IncS$_{Cm}$ harboring genetic elements to facilitate the insertion of a group II intron and the ß-lactamase gene at nucleotide position 412 of the *incS*$_{Cm}$ ORF (*intron-bla*, blue arrow). Step 3: Expression of IncS$_{Ct}$ from the complementation plasmid, allows for integration of the *intron-bla* cassette and interruption of the *incS*$_{Cm}$ ORF. (B) Single plane confocal micrographs of HeLa cells infected for 18h with the *Chlamydia muridarum ΔincS*$_{Cm}$*::bla* conditional mutant expressing mCherry (*incS*$_{Cm}$*::bla* pTet-IncS$_{Ct}$-3xFLAG, left panels, red) in the presence (+aTc, top panels) or the absence (-aTc, bottom panels) of aTc and stained with anti-FLAG antibody (IncS$_{Ct}$-3xFLAG, middle panels, green). The merge is shown on the right. Scale bar: 5μm. (C) Fold growth of wild-type *C. muridarum* (*Cm wt*) and the *Chlamydia muridarum ΔincS*$_{Cm}$*::bla* conditional mutant (*incS*$_{Cm}$*::bla* pTet-IncS$_{Ct}$) in HeLa cells at 39h pi compare to 0h pi in the presence (+aTc) or absence (-aTc) of aTc. Data are mean ± SEM, three combined experiments, One-way ANOVA, Tukey's Multiple Comparison Test, ** P<0.01 (-aTc vs + aTc); *** P<0.001 (-aTc vs wt).

https://doi.org/10.1371/journal.ppat.1010818.g003

absence of complementation, the *incS*$_{Cm}$*::bla* conditional mutant barely produced any infectious progeny, and displayed a 2- and 3-log reduction compared to the complemented and wild-type strains, respectively. Addition of aTc resulted in robust, yet partial complementation, with the complemented *incS*$_{Cm}$*::bla* mutant displaying a 1-log reduction in infectious progeny production compared to the wild-type strain. Thus, the critical role of IncS in establishing a productive infection in cell culture is conserved between *C. trachomatis* and *C. muridarum*.

IncS is required to initiate inclusion development *in vivo*

To determine if IncS is required for successful infection *in vivo*, C3H/HeJ female mice were intravaginally infected, and vaginal shedding was monitored every other day by swabbing the

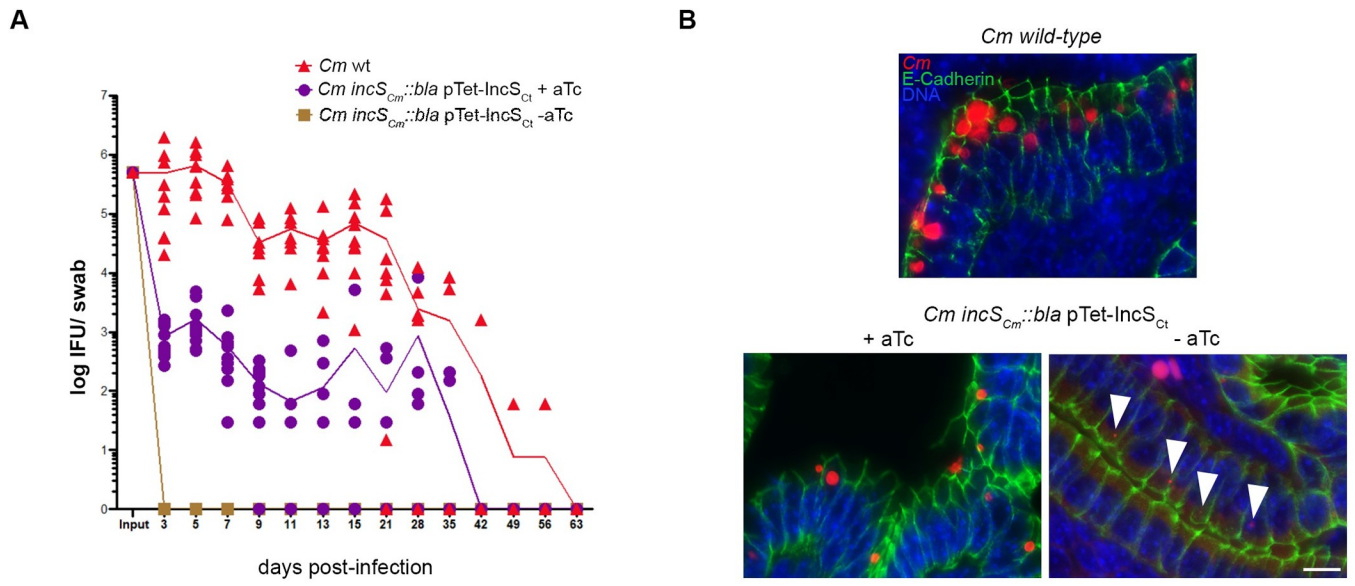

Fig 4. *In vivo* developmental defect of a *Chlamydia muridarum incS* conditional mutant. (A) Infectious progeny recovered at the indicated time from vaginal swabs after intravaginal inoculation of C3H/HeJ mice with wild-type *C. muridarum* (red triangles), or the *incS*$_{Cm}$::*bla* mutant complemented (purple circles) or not (brown squares) by addition of aTc to the drinking water. Each data point represents a mouse. Combined results from 2 independent experiments with 5 mice per group is shown. Mixed effect analysis with multiple comparisons and Tukey corrections: days 3–9 pi P<0.0001 (all groups), day 11 pi P = 0.0464 (complemented vs mutant), day 13 pi not significant (complemented vs mutant). (B) Fluorescence microscopy images of paraffin sections of endometrial epithelium of C3H/HeJ mice transcervically infected for 8h with wild-type *C. muridarum* (top panel), or the *incS*$_{Cm}$::*bla* mutant complemented (bottom left panel) or not (bottom right panel, arrowheads indicate intracellular bacteria) by addition of aTc to the drinking water and stained for DNA (blue), E-Cadherin (green) and *C. muridarum* (red). One representative mouse shown. Scale bar: 10μm.

https://doi.org/10.1371/journal.ppat.1010818.g004

vaginal vault and enumeration of live infectious bacteria (Fig 4A). In the absence of complementation, mice infected with the *incS*$_{Cm}$::*bla* conditional mutant did not shed infectious bacteria, compared to the sustained vaginal shedding of mice infected with wild-type bacteria. Mutant complementation, by addition of aTc in the drinking water of infected mice, led to a significant and sustained bacterial shedding, although shedding was not restored to wild-type levels. To further investigate inclusion development *in vivo*, mice were transcervically infected for 8h with wild-type bacteria, or with the *C. muridarum incS*$_{Cm}$::*bla* conditional mutant in the presence or absence of aTc in the drinking water. The genital tracts were excised, and infected cells were visualized on paraffin sections by *in situ* labelling of the bacteria and immunostaining of endometrial epithelial cells (Fig 4B). Large inclusions containing multiple bacteria were observed in the endometrial epithelium of mice infected with wild-type bacteria or the complemented mutant (+aTc). In line with the partial complementation of the vaginal shedding phenotype (Fig 4A), inclusions were smaller with the complemented strain than with wild-type bacteria. In contrast, in the absence of complementation (-aTc), infected endometrial cells only displayed single bacterium-containing inclusions (Fig 4B, arrowheads). Thus, the *C. muridarum incS*$_{Cm}$::*bla* conditional mutant displays a severe, yet complementable, colonization defect *in vivo*, which can be attributed to a defect in inclusion development.

Discussion

Identification of essential genes in obligate intracellular pathogens

Inactivation of essential genes is lethal and therefore prevents the amplification and isolation of the corresponding mutant. To overcome this challenge, we combined existing genetics tools for *Chlamydia* to generate targeted *C. trachomatis* and *C. muridarum* conditional mutants by

providing an inducible wild-type allele of the target gene in trans from a complementation plasmid, prior to replacing and interrupting the chromosomal allele with a selection cassette, respectively. Conditional knock-down *C. trachomatis* mutants, where expression of the gene of interest is downregulated using the CRISPRi methodology have been described before[24]; however, to our knowledge, this is the first report of a *Chlamydia* conditional knock-out mutant. Another major advance resulting from our study is the conditional expression of the complementation allele *in vivo*. Systemic delivery of inducers, such as doxycycline, is commonly used to generate inducible transgenic mice [25]. We have adapted this approach and shown that administration of aTc in the drinking water of mice was sufficient to yield enough inducer throughout the genital tract and therefore constitutes a viable option for mutant complementation *in vivo*. Overall, the technological advances described here to generate conditional mutants in *Chlamydia* are simple to implement and will benefit the characterization of the role of *Chlamydia* effectors in cell culture and *in vivo* as the field moves forward.

One question that remains to be addressed is how to ascertain that IncS is essential, versus highly important. The *C. trachomatis* $\Delta incS_{Ct}$ mutant was severely attenuated in cell culture and *in vivo*; however, serial passages in the absence of aTc in cell culture did not result in sterilization, instead the $\Delta incS_{Ct}$ mutant produced consistent low level of infectious progeny at each passage (not shown). This result could be due to the fact that *incS* is highly important rather than essential; however, leakiness of the Tet inducible promoter could also explain this phenotype. We cannot at this point distinguish between these two possibilities. Essentiality is supported by the fact, that, after many failed attempts, allelic exchange and/or interruption of the *incS* ORF was only achieved in the presence of complementation, both in *C. trachomatis* and *C. muridarum*. Additionally, albeit non-saturating, chemical mutagenesis in *C. trachomatis* and transposition mutagenesis in *C. trachomatis* or *C. muridarum* did not result in premature stop codons in $incS_{Ct}$ nor transposon insertion in $incS_{Ct}$ or $incS_{Cm}$ [26–28]. Moreover, although IncS-3xFLAG was not detected on the inclusion membrane in the absence of aTc, we cannot rule out that in some bacteria minute undetectable levels of IncS were sufficient to reach a certain threshold and rescued the developmental phenotype of the *incS* mutant. To settle *incS* essentiality, future studies are needed and will focus on improving the repression of the inducible promoter by combining aTc-dependent transcriptional regulation with a recently described riboswitch-dependent translational control [29]. A complementary approach will be to attempt to cure the complementation plasmid.

IncS (CTL0402/CT147/TC0424)

IncS is an Inc protein conserved in all *Chlamydiae*, including *C. trachomatis* serovar L2 (CTL0402), serovar D (CT147), and *C. muridarum* (TC0424) [10, 13, 30, 31]. IncS is expressed 1h post-infection and throughout the developmental cycle [30].

A role for CT147 in inclusion avoidance of the endocytic pathway was proposed based on computational analysis and CT147 homology to the human Early Endosomal Antigen 1 (EEA1) protein [30]. The authors did not experimentally validate their hypothesis, and we did not observe any co-localization between $\Delta incS_{Ct}$ mutant inclusions and EEA1 or LAMP1. Additionally, using currently available online software, we were not able to identify any region of homology between EEA1 and CT147, or its homologues.

Recently, a role for CTL0402 and TC0424 in inclusion integrity and preventing host cell death was proposed based on *C. trachomatis*/*C. muridarum* chimeric strains, generated by lateral gene transfer, in which distinct regions of the *C. trachomatis* serovar L2 chromosome is replaced with region of the *C. muridarum* chromosome [31]. More specifically, replacement of *C. trachomatis ctl0402* with *C. muridarum tc0424* led to the loss of CTL0402 in the inclusion

membrane, bacterial release into the host cell cytosol in mid-cycle, and an increase in the number of cells presenting hallmarks of apoptosis. Although strains with similar *C. trachomatis*/*C. muridarum* genetic make-up were compared and backcross experiments were performed, the phenotype was not complemented in trans, and it is unclear if the phenotype of the chimera is due to dysregulated TC0424 expression in a *C. trachomatis*/*C. muridarum* background.

Here using targeted mutagenesis and complemented strains, we were able to unequivocally link the genotype of *C. trachomatis* and *C. muridarum incS* mutants to a severe developmental defect in the early stages of the developmental cycle. Although *incS* mutant inclusions were negative for the endocytic pathway markers EEA1 and LAMP1, we cannot fully exclude mistrafficking of the inclusions, as proposed by Belland et al. Similarly, although the early developmental defect of the *incS* mutants was not associated with mid-stage inclusion rupture or cell death, we cannot at this stage rule out that perturbation of inclusion membrane integrity early in the developmental cycle contributes to the phenotype of the *incS* mutant.

Early *Chlamydia* development and EB to RB transition

The host and/or bacterial determinants that control each step of the *Chlamydia* developmental cycle, especially the EB to RB transition, are poorly characterized. The morphological difference between EB and RB is attributed to condensed and relaxed chromatin, respectively. The *Chlamydia* histone-like proteins Hc1 and Hc2 and a small metabolite of the non-mevalonate methylerythritol phosphate (MEP) pathway of isoprenoid biosynthesis are proposed to mediate DNA condensation [32, 33]. Proteomics profiling of EB and RB revealed significant differences, but none of these differences provided answers regarding the mechanism of EB to RB transition [34, 35]. Transcriptomic analysis of infected cells revealed that bacterial transcription is initiated as early as 1h pi and that bacterial genes are temporally expressed with transcription being initiated during the early (EB-RB transition), mid (RB replication) or late (RB-EB transition) stages of the developmental cycle [30, 36–41]. However, when investigating the genetic control of the initial step of the *Chlamydia* developmental cycle, there is very little, when any, overlap between the genes identified in the above referenced studies, most likely due to differences in approaches, timing of infection and normalization conditions. Additionally, except for the study by Rajeeve et al implicating glutamine uptake as a critical step for peptidoglycan synthesis and initiation of the EB conversion to RB [41], to date none of the candidates identified by transcriptomics have been validated to play a role in *Chlamydia* development in the context of infection, leaving the molecular mechanisms supporting EB to RB transition uncharacterized.

Our results indicate that IncS mutant bacteria are impaired in EB to RB transition during the early stages of *Chlamydia* development and that IncS function is conserved in *C. trachomatis* and *C. muridarum*. We do note that, under the conditions tested here, the *C. trachomatis* $incS_{Ct}$ allele did not fully complement the phenotype of the *C. muridarum* mutant, perhaps because $IncS_{Ct}$ and $IncS_{Cm}$ only share 60% identity (76% similarity), which may result in suboptimal interaction with target protein(s). The partial complementation observed *in vivo* could also be due to the additive effect of a low final aTc concentration in the genital tract. Future studies will focus on elucidating how a single inclusion membrane protein contributes to successful progression through the early stages of the *Chlamydia* developmental cycle by potentially controlling the transcriptional reprogramming of infectious EB bacteria into replicative RB and/or remodeling the nascent inclusions into a replicative niche.

Conclusion

In an attempt to overcome gene essentiality in obligate intracellular pathogens, we have adapted available genetic tools to generate conditional mutants in *C. trachomatis* and *C.*

muridarum. The method for efficient *in vivo* complementation of a conditional mutant described here will be instrumental in applying the molecular Koch's postulates when characterizing pathogenic properties of *Chlamydia* effector proteins [42]. Additionally, because *incS* is a *Chlamydia spp*.-specific gene expressed during human infections [43, 44] but absent from other bacterial species, including members of the microbiota, IncS is an ideal target for the development of antibiotics that would specifically inhibit *Chlamydia* development during infection.

Material and methods

Ethics statement

All genetic manipulations and containment work were approved by the University of Virginia (UVA) Biosafety Committee and are in compliance with the section III-D-1-a of the National Institute of Health guidelines for research involving recombinant DNA molecules. All animal experiments were approved by the UVA Institutional Animal Care and Use Committee.

Cell lines and bacterial strains

HeLa cells (CCL-2) were obtained from ATCC and cultured at 37˚C with 5% CO2 in high-glucose Dulbecco's modified Eagle's medium (DMEM; Invitrogen) supplemented with 10% heat-inactivated fetal bovine serum (Invitrogen). *C. trachomatis* lymphogranuloma venereum (LGV) type II was obtained from the ATCC (L2/434/Bu VR-902B). *C. muridarum* Nigg was obtained from Michael Starnbach (Harvard Medical School, Boston, MA). *C. trachomatis* and *C. muridarum* expressing mCherry under the control of the *groESL* promoter were described previously [21]. Chlamydia propagation, infection and transformation were performed as previously described [21, 45]. All *Chlamydia* strains were plaque purified.

Plasmid construction

Restriction enzymes and T4 DNA ligase were obtained from New England BioLabs (Ipswich, MA). PCR was performed using Herculase DNA polymerase (Stratagene). PCR primers were obtained from Integrated DNA Technologies. Primers and cloning strategies are described in S1 Table and detailed below.

Construction of pSU-ΔIncS

The plasmid was constructed via the Gibson assembly using HiFi DNA assembly master mix (New England Biolabs) following manufacturer instructions. 3-kb fragments downstream and upstream of *incS* (PCR A, right arm and PCR B, left arm, respectively) were amplified from *C. trachomatis* L2 genomic DNA via PCR using primers pSUmC3Dwn0402 5 2.1 and 3Dwn0402pSumC 3 2.1 and pSUmC3Up0402 5 and 3Up0402pSUmC 3, respectively. PCR A and PCR B were sequentially cloned into the SbfI and SalI sites of pSUmC-4.0, respectively, so that each arm immediately flanked the *aadA-gfp* cassette [46].

Construction of pSW2-TetIncS$_{Ct}$

DNA fragments corresponding to the *tet* repressor (*tetR*), *tetA* promoter ($tetA^P$) (PCR A) and to the 3xFLAG and the *incDEFG* operon terminator (PCR C) were amplified by PCR from p2TK2-SW2 mCh(Gro) Tet-IncV-3F plasmid [47] using primers TetRSTOP5Kpn and TetA-P-IncS Rv, and 0402FLAG Fw and IncDTerm3Not, respectively. A DNA fragment corresponding to the *ctl0402* ORF (PCR B) was amplified from *C. trachomatis* L2 genomic DNA by PCR using primers TetAP-IncS Fw and 0402 FLAG Rv. A DNA fragment corresponding to

TetR-tetAP CTL0402 3xFLAG *incDEFG* terminator (PCR D) was amplified by overlapping PCR using PCR A, B and C as template and primers TetRSTOP5Kpn and IncDTerm3Not. A DNA fragment (PCR E) corresponding to *Neisseria meningitidis* promoter-GFP (nmP-GFP) was amplified by PCR from pGFP::SW2 [48] with primers AgeI nmP Prom Fw and RSGFP TAA AgeI Rv. Fragment D and E were sequentially cloned into the KpnI/NotI sites and AgeI site, respectively, of p2TK2$_{Amp}$-SW2 [49].

Construction of pNigg-TetIncS$_{Ct}$

The DNA fragment corresponding to TetR-tetA^{P} CTL0402 3xFLAG *incDEFG* terminator was obtained by KpnI/NotI digest of pSW2-TetIncS$_{Ct}$ and cloned into p2TK2$_{Spec}$-Nigg mCh (Gro$_{L2}$) [21].

Construction of pDFTT3-IncS$_{Cm}$

The GrpII intron was retargeted for *tc0424* (IncS$_{Cm}$) using primers TC0424-412 IBS1/2, TC0424-412 EBS1/delta, and TC0424-412 EBS2 designed by the TargeTron computer algorithm (TargeTronics). The resulting PCR product was digested with BsrGI and HindIII and cloned into the BsrGI/HindIII site of the pDFTT3-*bla*-IncA suicide vector [19].

Validation of *Ct* ΔincS$_{Ct}$ pTet-IncS$_{Ct}$

Allelic exchange of the *incS* ORF with the *aadA-gfp* cassette was confirmed by PCR (S1 Fig and S1 Table). WT and *ΔincS$_{Ct}$* pTet-IncS$_{Ct}$ genomic DNA, prepared using illustra bacteria genomicPrep Mini Spin Kit (GE Healthcare), according the manufacturer recommendations, were used as template in PCR reactions using two sets of primers surrounding the 3kb homology recombination site (incS 3kb Up Fw & incS 3kb Dwn Rv) or surrounding the *incS* ORF (incS Up Fw & incS Dwn Rv). The PCR products were run into 1% agarose gel, stained with ethidium bromide, and viewed using UV transillumination. The PCR products were extracted from the agarose gel using QIAquick Gel Extraction Kit (Qiagen) and sequenced via Sanger performed by Genscript.

The conditional expression and inclusion localization of IncS$_{Ct}$ was validated by immunofluorescence. HeLa cells seeded on glass coverslips were infected with *Ct* ΔincS$_{Ct}$ pTet-IncS$_{Ct}$ in the presence of 0.5ng/ml aTc (+aTc) or not (-aTc) for 24 h, fixed stained with mouse monoclonal anti-FLAG (1:1,000; Sigma) and secondary antibodies (Alexa Fluor 594-conjugated goat anti-mouse antibody (1:500; Molecular Probes) and processed for confocal microscopy.

Validation of *Cm incS$_{Cm}$*::*bla* pTet-IncS$_{Ct}$

Intron integration and interruption of the *tc0424* (*incSC$_m$*) ORF was confirmed by PCR using genomic DNA and primers TC0424 Ups Fw and TC0424 (691–719) Rv, which flank the insertion site of the intron (S4 Fig and S1 Table). The PCR products amplified from mutant genomic DNA showed the expected 2 kb increase in band size compare to wild-type.

The conditional expression and inclusion localization of IncS$_{Ct}$ was validated by immunofluorescence as described for *Ct* ΔincS$_{Ct}$ pTet-IncS$_{Ct}$, except that infection was performed in the presence of 1ng/ml aTc.

Immunofluorescence and confocal microscopy

All steps were performed at room temperature. At the indicated times, cells were fixed with 4% paraformaldehyde in 1× PBS for 30 min and sequentially incubated with primary and

secondary antibodies diluted in 0.1% Triton X-100 in 1× PBS for 1h or with the DNA dye 7AAD-red. Coverslips were washed with 1× PBS and mounted with DABCO antifade-containing mounting medium. Confocal microscopy was performed using the Leica DMi8 microscope equipped with the Andor iXon ULTRA 888BV EMCCD camera and the confocal scanner unit CSU-W1, and driven by the IQ software. Images were processed using the Imaris software (Bitplane, Belfast, United Kingdom).

Infectious progeny production

HeLa cells seeded in 96 well plates were infected with the *C. trachomatis* or *C. muridarum incS* conditional mutant at an MOI of 0.5 in medium containing 0.5ng/ml of aTc or at an MOI of 10 without aTc. Infection was synchronized by centrifugation for 10 min at 600g. Cells were lysed at 0h and 48h (*C. trachomatis*) or 39h (*C. muridarum*) post infection in 100μl sterile water, and 5-fold dilutions of the lysates were used to infect fresh HeLa cell monolayers seeded in 384 well plates in the presence of aTc. At 24h pi cells were fixed with 4% paraformaldehyde in 1x PBS. Infected cells were stained with Hoechst. Quantification of inclusion forming units (IFUs) per ml using the MetaXpress software. Fold growth was determined as the ratio between IFUs/ml at 48h (*C. trachomatis*) or 39h (*C. muridarum*) pi/0h pi.

Percentage of cells with an inclusion upon addition or removal of aTc at different time post infection

HeLa cells seeded in 96 well black plates were infected with the *C. trachomatis* $\Delta incS_{Ct}$ conditional mutant at an MOI of 1 in the absence (Fig 2A) or the presence of 0.5ng/ml of aTc (Fig 2B). Infection was synchronized by centrifugation for 10 min at 600g. Cells were washed 5 times with 200 μl of DMEM at 2, 4, 6 or 8h pi and the medium was replaced with 0.5ng/ml aTc (Fig 2A) or without aTc (Fig 2B). The cells were fixed with 4% paraformaldehyde in 1x PBS at 28h pi. Infected cells were stained with Hoechst. The percentage of infection was determined using the MetaXpress software.

Intracellular localization and morphology of the *C. trachomatis incS* conditional mutant

HeLa cells seeded on glass coverslips were infected with the *C. trachomatis* $\Delta incS_{Ct}$ conditional mutant at an MOI of 10 in the presence of 0.5ng/ml aTc, absence aTc, or with aTc added at 4h pi. Infection was synchronized by centrifugation for 10 min at 600g. At 2h pi cells were washed 5 times with 500 μl of DMEM to remove the non-infectious bacteria and the medium was replaced. At 12h pi samples were fixed with 4% paraformaldehyde stained with the DNA dye 7AAD-red and processed and imaged by confocal microscopy. The number of total intracellular bacteria (as determined by bacteria that were in the same focal plane as the nuclei) and RB (as determine by bacteria of about 1 μm in diameter with the Imaris software) per cell were quantified manually with the Imaris Imaging software. 150 infected cells were analyzed per sample.

Electron microscopy

HeLa cells were infected with the *C. trachomatis* $\Delta incS_{Ct}$ conditional mutant in the presence of 0.5ng/ml aTc (+aTc) or not (-aTc) at an MOI of 15. Infection was synchronized by centrifugation for 10 min at 600g. Twelve hours post-infection, the samples were fixed in 2.5% glutaraldehyde in 0.1 M cacodylate buffer (pH 7.4) for 60 min at RT. After fixation, cells were scraped off and pelleted, as described previously [50]. Ultrathin sections of infected cells were stained

with osmium tetraoxide before examination with Hitachi 7600 EM under 80 kV equipped with a dual AMT CCD camera system.

Quantification of OmcA levels

HeLa cells seeded on coverslips were infected with the *C. trachomatis* $\Delta incS_{Ct}$ conditional mutant at an MOI of 15 in the presence of 0.5ng/ml aTc or absence of aTc. At 6h and 12 hpi, the cells were processed for immunofluorescence and confocal microscopy as described above, except that 0.2% Triton X-100 was used for permeabilization and immunostaining. OmcA was detected using rabbit polyclonal anti-OmcA antibodies [21] (1 in 200 in 0.2% Triton X-100 in 1× PBS over-night at 4˚C), followed by Alexa Fluor 594-conjugated goat anti-rabbit antibody (1:500; Molecular Probes) and the DNA dye SytoxGreen (1:50,000; Invitrogen), both diluted in 0.1% Triton X-100 in 1× PBS and incubated at room temperature for 1h. After confocal imaging, the levels of OmcA associated with perinuclear bacteria were quantified as described below and in S3 Fig. The baseline background was subtracted for each channel (green for DNA, red for OmcA) (Step 1). For each infected cell, a surface area containing the bacteria clustered at the perinuclear region of the cell was manually created in every other XY plane of merge images (Step 2). A 3D object combining the surface areas from step 2, and the intercalating XY planes, was generated (Step 3). The sum intensity of the OmcA and DNA signal within the 3D object from step 3 was recorded (Step 4). The OmcA levels, in arbitrary units, were determined by normalizing the sum intensity of the OmcA signal with the sum intensity of DNA signal (Step 5). For each condition, a total of 30 infected cells were quantified. Infected cells where the bacteria were overlapping with the host nucleus or with another infected cell were excluded from the analysis.

Intravaginal infections and vaginal shedding

Six-to-eight-week-old female C3H/HeJ mice (The Jackson Laboratory) were treated subcutaneously with 2.5 mg medroxyprogesterone acetate (Depo-Provera, Pfizer) 7 days prior to infection. When indicated, aTc (10μg/ml final) was added to the drinking water 4 days prior to infection and for the duration of the experiment. aTc treated water was kept in amber bottles and replaced every other day. In a pilot experiment, final concentration of aTc in the drinking water of 100μg/ml or 10μg/ml resulted in similar complementation. Testing higher concentrations were cost-prohibitive (at least when providing fresh water every other day). We did not test lower concentrations or try replacing the water less frequently. To monitor vaginal shedding, $5x10^5$ IFUs of the indicated *C. muridarum* strain were introduced in the vaginal vault (5 mice per group). Shedding was monitored every other day by swabbing the vaginal vault. Each swab was collected in 500 μl of cold SPG with glass beads and vortexed vigorously. The released bacteria were serially diluted in SPG and titrated on HeLa cell monolayers in medium containing 2.5 μg/ml Amphotericin B (Gibco), 50 μg/ml gentamycin (Gibco), and 1 ng/ml aTc. At 18h pi, the number of inclusions for each condition was enumerated based on mCherry expression and used to calculate log IFUs/ml. Mice were swabbed until the infection was cleared, as determined by 2 consecutive negative swabs.

Transcervical infections and tissue preparation for microscopy

To visualize *C. muridarum* infected cells *in vivo*, $5x10^5$ IFUs were delivered directly into the uterine horn of six-to-eight-week-old female C3H/HeJ mice (The Jackson Laboratory), using a non-surgical embryo transfer device (ParaTechs Corp) (3 mice per group). Mice were pretreated with 2.5 mg medroxyprogesterone acetate (Depo-Provera, Pfizer) 7 days prior to infection. When indicated, aTc was added to the drinking water as described for intravaginal

infections. The mice were sacrificed at 8h pi. The genital tracts were excised and placed into histology cassettes. The cassettes were immersed in 10% formalin for 48h. The tissues were preserved in 70% ethanol before loading onto a tissue processor for dehydration and paraffin infiltration. After manual embedding into a paraffin block, paraffin sections were cut at 5 μm on a Leica microtome.

Microscopy of infected tissue

Paraffin sections were deparaffinized and dehydrated in the following sequence: xylene, 100% ethanol, and hydrogen peroxide. Antigen retrieval was performed at 95–100˚C for 15 min using boiling 1x RNAscope Target Retrieval Reagent (Advanced Cell Diagnostics, 322000). Slides were rinsed in deionized water for 15 seconds and washed in 100% ethanol for 3 min.

Slides were permeabilized with RNAscope Protease Plus for 30 min at 40˚C within the RNAscope HybEZ II Hybridization System. Slides were washed in RNAscope Wash Buffer (Advanced Cell Diagnostics, 310091). The *C. muridarum*-23srRNA-C1 probe (Advanced Cell Diagnostics, 1039531-C1) was hybridized on the slides for 2 h at 40˚C within the RNAscope HybEZ II System. Slides were washed in RNAscope Wash Buffer. Slides were incubated within the RNAscope HybEZ II System using the RNAscope Multiplex Fluorescent Detection Reagents v2 kit (Advanced Cell Diagnostics, 323110) in order at 40˚C: AMP 1 (Advanced Cell Diagnostics, 323101) for 30 min, AMP 2 (Advanced Cell Diagnostics, 323102) for 30 min, AMP 3 (Advanced Cell Diagnostics, 323103) for 15 min, HRP-C1 (Advanced Cell Diagnostics, 323104) for 15 min, Opal 690 Reagent (Akoya Biosciences, OP-001006) at 1:1000 within RNAscope Multiplex TSA Buffer (Advanced Cell Diagnostics, 322809) for 30 min, and HRP blocker (Advanced Cell Diagnostics, 323107) for 15 min. After each incubation step, slides were washed in RNAscope Wash Buffer for 5 min with gentle agitation.

Immediately following RNAscope procedure, slides were blocked with 2% normal goat serum in 5% Bovine Serum Albumin (AmericanBio, AB01088-00100) PBS for 1 h at room temperature. Primary antibodies were diluted 1:100 in blocking buffer (E-cadherin, BD Biosciences 610181) and incubated overnight at RT. Secondary antibodies (goat anti-mouse Alexa Fluor 488,) were diluted 1:500 in blocking buffer and incubated for 2 h at room temperature. Slides were counterstained using RNAscope Multiplex FL v2 DAPI (Advanced Cell Diagnostics, 323108) for 1 min. Coverslips were mounted using ProLong Gold Antifade Mountant (Thermo Fisher Scientific, P36930). Slides were imaged using a Nikon TE2000 microscope equipped for automated multi-color imaging including motorized stage and filter wheels, a Hamamatsu Orca ER Digital CCD Camera and piezo-driven ×10 objective. The corresponding images were processed with the MetaMorph software (Molecular Devices, Inc.).

Statistics

Except when noted, each experiment was performed in triplicate, and the average and SEM from one representative experiment are shown. The graphs were generated using GraphPad Prism. The appropriate statistical tests were used and are indicated in the Figure legends.

Supporting information

S1 Fig. Validation of the *Chlamydia trachomatis incS* conditional mutant. (A) Schematic representation of the $incS_{Ct}$ locus of wild-type (WT) and Δ$incS_{Ct}$ mutant *C. trachomatis* strains and of the primers used for mutant validation by PCR. P1 (incS 3kb Up Fw), P2 (incS 3kb Dwn Rv), P3 (incS Up Fw), P4 (incS Dwn Rv). (B) DNA gels of PCR products generated using the following combination of genomic DNA template/primer, as described in (A). Left panel: WT/P1P2 (lane 2) and Δ$incS_{Ct}$/P1P2 (lane 3). Right panel: WT/P3P4 (lane 2) and Δ$incS_{Ct}$/

P3P4 (lane 3). The ladder is shown in lane 1.
(TIF)

S2 Fig. Ultrastructural analysis of *Chlamydia trachomatis incS* conditional mutant bacteria. Transmission electron micrographs of sections of HeLa cells infected with a *C. trachomatis* Δ$incS_{Ct}$ *conditional* mutant at an MOI of 15 for 12h in the presence (+aTc) or absence (-aTc) of aTc. RB: Reticulate Body; IB: Intermediate Body. Scale bar: 1 μm.
(TIF)

S3 Fig. Method to quantify the levels of OmcA associated with perinuclear bacteria. Step 1: The baseline background was subtracted for each channel (green for DNA, red for OmcA) Step 2: For each infected cell, a surface area containing the bacteria clustered at the perinuclear region of the cell was manually created in every other XY plane. Step 3: A 3D object was generated combining the surface areas from step 2. Step 4: The sum intensity of the OmcA and DNA signal within the 3D object from step 3 was recorded: Step 5: The OmcA levels, in arbitrary units, was determined by normalizing the Sum intensity of the OmcA signal with the Sum intensity of DNA signal.
(TIF)

S4 Fig. Validation of the *Chlamydia muridarum incS* conditional mutant. (A) Schematic representation of the $incS_{Cm}$ locus of wild-type (WT) and $incS_{Cm}$::*bla* mutant *C. muridarum* strains, and of the primers used for mutant validation by PCR. P1 (TC0424 Up Fw), P2 (TC0424 (691–719)). (B) DNA gels of PCR products generated using the following combination of genomic DNA template/primer, as described in (A). WT/P1P2 (lane 2) and $incS_{Cm}$::*bla*/P1P2 (lane 3). The ladder is shown in lane 1. (C) The site of insertion of the group II intron was confirmed by Sanger sequencing. A translation of the resulting IncSCm truncated peptide is presented. The asterisk denotes the early stop codon introduced by the insertion of the group II intron (brown: $IncS_{Cm}$, blue: group II intron).
(TIF)

S1 Table. Primers pairs (name and sequence) and corresponding templates used in this study.
(XLSX)

S1 Data set. Raw data from Fig 1.
(XLSX)

S2 Data set. Raw data from Fig 2.
(XLSX)

S3 Data set. Raw data from Fig 3.
(XLSX)

S4 Data set. Raw data from Fig 4.
(XLSX)

Acknowledgments

We thank members of the Derré laboratory for providing feedback on the project and the manuscript. We thank Drs. Ken Field for helpful discussions and advices to generate the FRAEM conditional mutant; the excellent technical staff of the Electron Microscopy Core Facility at the Johns Hopkins University School of Medicine Microscopy Facility; Drs. Michael Starnbach, Rodrigo Gonzalez, and Jen Helble (Harvard Medical School), and Drs. Melanie

Rutkowski, and Kumari Andarawewa (UVA) for advice on animal handling, the murine model of *Chlamydia* infection, and transcervical infections; Homer Ransdell and the UVA Fontaine Vivarium staff for assistance with animal work; Sheri Vanhoose and the UVA Research Histology Core for preparing paraffin sections; and Dr. Hervé Agaisse for providing expertise with tissue processing, the RNAscope methodology, and comments and discussion on the manuscript.

Author Contributions

Conceptualization: María Eugenia Cortina, R. Clayton Bishop, Isabelle Derré.

Formal analysis: María Eugenia Cortina, R. Clayton Bishop, Isabelle Coppens, Isabelle Derré.

Funding acquisition: Isabelle Coppens, Isabelle Derré.

Investigation: María Eugenia Cortina, R. Clayton Bishop, Brittany A. DeVasure, Isabelle Coppens, Isabelle Derré.

Methodology: María Eugenia Cortina, R. Clayton Bishop, Isabelle Derré.

Project administration: Isabelle Derré.

Supervision: Isabelle Derré.

Validation: María Eugenia Cortina, R. Clayton Bishop, Isabelle Derré.

Visualization: María Eugenia Cortina, R. Clayton Bishop, Isabelle Coppens, Isabelle Derré.

Writing – original draft: María Eugenia Cortina, Isabelle Derré.

Writing – review & editing: María Eugenia Cortina, R. Clayton Bishop, Isabelle Coppens, Isabelle Derré.

References

1. CDC. STI Prevalence, Incidence, and Cost Estimates in the United States 2021.
2. Newman L, Rowley J, Vander Hoorn S, Wijesooriya NS, Unemo M, Low N, et al. Global Estimates of the Prevalence and Incidence of Four Curable Sexually Transmitted Infections in 2012 Based on Systematic Review and Global Reporting. PLoS One. 2015; 10(12):e0143304. Epub 2015/12/10. https://doi.org/10.1371/journal.pone.0143304 PMID: 26646541; PubMed Central PMCID: PMC4672879.
3. Haggerty CL, Gottlieb SL, Taylor BD, Low N, Xu F, Ness RB. Risk of sequelae after Chlamydia trachomatis genital infection in women. J Infect Dis. 2010;201 Suppl 2:S134–55. Epub 2010/05/28. https://doi.org/10.1086/652395 PMID: 20470050.
4. Starnbach MN. Action Needed on Chlamydia Vaccines. Trends Microbiol. 2018; 26(8):639–40. Epub 2018/06/03. https://doi.org/10.1016/j.tim.2018.05.006 PMID: 29858127.
5. de la Maza LM, Darville TL, Pal S. Chlamydia trachomatis vaccines for genital infections: where are we and how far is there to go? Expert Rev Vaccines. 2021; 20(4):421–35. Epub 2021/03/09. https://doi.org/10.1080/14760584.2021.1899817 PMID: 33682583.
6. Moulder JW. Interaction of chlamydiae and host cells in vitro. Microbiol Rev. 1991; 55(1):143–90. Epub 1991/03/01. https://doi.org/10.1128/mr.55.1.143-190.1991 PMID: 2030670; PubMed Central PMCID: PMC372804.
7. Grieshaber SS, Grieshaber NA, Hackstadt T. Chlamydia trachomatis uses host cell dynein to traffic to the microtubule-organizing center in a p50 dynamitin-independent process. J Cell Sci. 2003; 116(Pt 18):3793–802. Epub 2003/08/07. https://doi.org/10.1242/jcs.00695 PMID: 12902405.
8. Moore ER, Ouellette SP. Reconceptualizing the chlamydial inclusion as a pathogen-specified parasitic organelle: an expanded role for Inc proteins. Front Cell Infect Microbiol. 2014; 4:157. https://doi.org/10.3389/fcimb.2014.00157 PMID: 25401095; PubMed Central PMCID: PMC4215707.
9. Bugalhao JN, Mota LJ. The multiple functions of the numerous Chlamydia trachomatis secreted proteins: the tip of the iceberg. Microb Cell. 2019; 6(9):414–49. Epub 2019/09/19. https://doi.org/10.15698/mic2019.09.691 PMID: 31528632; PubMed Central PMCID: PMC6717882.

10. Li Z, Chen C, Chen D, Wu Y, Zhong Y, Zhong G. Characterization of fifty putative inclusion membrane proteins encoded in the *Chlamydia trachomatis* genome. Infect Immun. 2008; 76(6):2746–57. Epub 2008/04/09. https://doi.org/10.1128/IAI.00010-08 PMID: 18391011; PubMed Central PMCID: PMC2423075.

11. Dehoux P, Flores R, Dauga C, Zhong G, Subtil A. Multi-genome identification and characterization of chlamydiae-specific type III secretion substrates: the Inc proteins. BMC Genomics. 2011; 12:109. https://doi.org/10.1186/1471-2164-12-109 PMID: 21324157; PubMed Central PMCID: PMC3048545.

12. Lutter EI, Barger AC, Nair V, Hackstadt T. *Chlamydia trachomatis* inclusion membrane protein CT228 recruits elements of the myosin phosphatase pathway to regulate release mechanisms. Cell Rep. 2013; 3(6):1921–31. https://doi.org/10.1016/j.celrep.2013.04.027 PMID: 23727243; PubMed Central PMCID: PMC3700685.

13. Weber MM, Bauler LD, Lam J, Hackstadt T. Expression and localization of predicted inclusion membrane proteins in *Chlamydia trachomatis*. Infect Immun. 2015; 83(12):4710–8. Epub 2015/09/30. https://doi.org/10.1128/IAI.01075-15 PMID: 26416906; PubMed Central PMCID: PMC4645406.

14. Mirrashidi KM, Elwell CA, Verschueren E, Johnson JR, Frando A, Von Dollen J, et al. Global Mapping of the Inc-Human Interactome Reveals that Retromer Restricts *Chlamydia* Infection. Cell Host Microbe. 2015; 18(1):109–21. https://doi.org/10.1016/j.chom.2015.06.004 PMID: 26118995; PubMed Central PMCID: PMC4540348.

15. Rahnama M, Fields KA. Transformation of Chlamydia: current approaches and impact on our understanding of chlamydial infection biology. Microbes Infect. 2018; 20(7–8):445–50. Epub 2018/02/08. https://doi.org/10.1016/j.micinf.2018.01.002 PMID: 29409975; PubMed Central PMCID: PMC6070436.

16. Sixt BS, Bastidas RJ, Finethy R, Baxter RM, Carpenter VK, Kroemer G, et al. The Chlamydia trachomatis Inclusion Membrane Protein CpoS Counteracts STING-Mediated Cellular Surveillance and Suicide Programs. Cell Host Microbe. 2017; 21(1):113–21. Epub 2017/01/04. https://doi.org/10.1016/j.chom.2016.12.002 PMID: 28041929; PubMed Central PMCID: PMC5233594.

17. Weber MM, Lam JL, Dooley CA, Noriea NF, Hansen BT, Hoyt FH, et al. Absence of Specific *Chlamydia trachomatis* Inclusion Membrane Proteins Triggers Premature Inclusion Membrane Lysis and Host Cell Death. Cell Rep. 2017; 19(7):1406–17. https://doi.org/10.1016/j.celrep.2017.04.058 PMID: 28514660.

18. Nguyen PH, Lutter EI, Hackstadt T. Chlamydia trachomatis inclusion membrane protein MrcA interacts with the inositol 1,4,5-trisphosphate receptor type 3 (ITPR3) to regulate extrusion formation. PLoS Pathog. 2018; 14(3):e1006911. Epub 2018/03/16. https://doi.org/10.1371/journal.ppat.1006911 PMID: 29543918; PubMed Central PMCID: PMC5854415.

19. Johnson CM, Fisher DJ. Site-specific, insertional inactivation of incA in Chlamydia trachomatis using a group II intron. PLoS One. 2013; 8(12):e83989. Epub 2014/01/07. https://doi.org/10.1371/journal.pone.0083989 PMID: 24391860; PubMed Central PMCID: PMC3877132.

20. Mueller KE, Wolf K, Fields KA. Gene Deletion by Fluorescence-Reported Allelic Exchange Mutagenesis in Chlamydia trachomatis. mBio. 2016; 7(1):e01817–15. Epub 2016/01/21. https://doi.org/10.1128/mBio.01817-15 PMID: 26787828; PubMed Central PMCID: PMC4725004.

21. Cortina ME, Ende RJ, Bishop RC, Bayne C, Derre I. Chlamydia trachomatis and Chlamydia muridarum spectinomycin resistant vectors and a transcriptional fluorescent reporter to monitor conversion from replicative to infectious bacteria. PLoS One. 2019; 14(6):e0217753. Epub 2019/06/07. https://doi.org/10.1371/journal.pone.0217753 PMID: 31170215; PubMed Central PMCID: PMC6553856.

22. Dockterman J, Coers J. Immunopathogenesis of genital Chlamydia infection: insights from mouse models. Pathog Dis. 2021; 79(4). Epub 2021/02/05. https://doi.org/10.1093/femspd/ftab012 PMID: 33538819; PubMed Central PMCID: PMC8189015.

23. O'Meara CP, Andrew DW, Beagley KW. The mouse model of Chlamydia genital tract infection: a review of infection, disease, immunity and vaccine development. Curr Mol Med. 2014; 14(3):396–421. Epub 2013/10/10. https://doi.org/10.2174/1566524013136660078 PMID: 24102506.

24. Ouellette SP, Blay EA, Hatch ND, Fisher-Marvin LA. CRISPR Interference To Inducibly Repress Gene Expression in Chlamydia trachomatis. Infect Immun. 2021; 89(7):e0010821. Epub 2021/04/21. https://doi.org/10.1128/IAI.00108-21 PMID: 33875479; PubMed Central PMCID: PMC8373233.

25. Saunders TL. Inducible transgenic mouse models. Methods Mol Biol. 2011; 693:103–15. Epub 2010/11/17. https://doi.org/10.1007/978-1-60761-974-1_7 PMID: 21080277.

26. Kokes M, Dunn JD, Granek JA, Nguyen BD, Barker JR, Valdivia RH, et al. Integrating chemical mutagenesis and whole-genome sequencing as a platform for forward and reverse genetic analysis of Chlamydia. Cell Host Microbe. 2015; 17(5):716–25. Epub 2015/04/30. https://doi.org/10.1016/j.chom.2015.03.014 PMID: 25920978; PubMed Central PMCID: PMC4418230.

27. LaBrie SD, Dimond ZE, Harrison KS, Baid S, Wickstrum J, Suchland RJ, et al. Transposon Mutagenesis in Chlamydia trachomatis Identifies CT339 as a ComEC Homolog Important for DNA Uptake and

Lateral Gene Transfer. mBio. 2019; 10(4). Epub 2019/08/08. https://doi.org/10.1128/mBio.01343-19 PMID: 31387908; PubMed Central PMCID: PMC6686042.

28. Wang Y, LaBrie SD, Carrell SJ, Suchland RJ, Dimond ZE, Kwong F, et al. Development of Transposon Mutagenesis for Chlamydia muridarum. J Bacteriol. 2019; 201(23). Epub 2019/09/11. https://doi.org/10.1128/JB.00366-19 PMID: 31501283; PubMed Central PMCID: PMC6832062.

29. Grieshaber NA, Chiarelli TJ, Appa CR, Neiswanger G, Peretti K, Grieshaber SS. Translational gene expression control in Chlamydia trachomatis. PLoS One. 2022; 17(1):e0257259. Epub 2022/01/28. https://doi.org/10.1371/journal.pone.0257259 PMID: 35085261; PubMed Central PMCID: PMC8794103.

30. Belland RJ, Zhong G, Crane DD, Hogan D, Sturdevant D, Sharma J, et al. Genomic transcriptional profiling of the developmental cycle of *Chlamydia trachomatis*. Proc Natl Acad Sci U S A. 2003; 100 (14):8478–83. Epub 2003/06/20. https://doi.org/10.1073/pnas.1331135100 PMID: 12815105; PubMed Central PMCID: PMC166254.

31. Dimond ZE, Suchland RJ, Baid S, LaBrie SD, Soules KR, Stanley J, et al. Inter-species lateral gene transfer focused on the Chlamydia plasticity zone identifies loci associated with immediate cytotoxicity and inclusion stability. Mol Microbiol. 2021. Epub 2021/11/06. https://doi.org/10.1111/mmi.14832 PMID: 34738268.

32. Grieshaber NA, Fischer ER, Mead DJ, Dooley CA, Hackstadt T. Chlamydial histone-DNA interactions are disrupted by a metabolite in the methylerythritol phosphate pathway of isoprenoid biosynthesis. Proc Natl Acad Sci U S A. 2004; 101(19):7451–6. Epub 2004/05/05. https://doi.org/10.1073/pnas.0400754101 PMID: 15123794; PubMed Central PMCID: PMC409939.

33. Grieshaber NA, Sager JB, Dooley CA, Hayes SF, Hackstadt T. Regulation of the *Chlamydia trachomatis* histone H1-like protein Hc2 is IspE dependent and IhtA independent. J Bacteriol. 2006; 188 (14):5289–92. Epub 2006/07/04. https://doi.org/10.1128/JB.00526-06 PMID: 16816202; PubMed Central PMCID: PMC1539943.

34. Saka HA, Thompson JW, Chen YS, Kumar Y, Dubois LG, Moseley MA, et al. Quantitative proteomics reveals metabolic and pathogenic properties of Chlamydia trachomatis developmental forms. Mol Microbiol. 2011; 82(5):1185–203. Epub 2011/10/22. https://doi.org/10.1111/j.1365-2958.2011.07877.x PMID: 22014092; PubMed Central PMCID: PMC3225693.

35. Skipp PJ, Hughes C, McKenna T, Edwards R, Langridge J, Thomson NR, et al. Quantitative Proteomics of the Infectious and Replicative Forms of Chlamydia trachomatis. PLoS One. 2016; 11(2):e0149011. Epub 2016/02/13. https://doi.org/10.1371/journal.pone.0149011 PMID: 26871455; PubMed Central PMCID: PMC4752267.

36. Shaw EI, Dooley CA, Fischer ER, Scidmore MA, Fields KA, Hackstadt T. Three temporal classes of gene expression during the *Chlamydia trachomatis* developmental cycle. Mol Microbiol. 2000; 37 (4):913–25. Epub 2000/09/06. https://doi.org/10.1046/j.1365-2958.2000.02057.x PMID: 10972811.

37. Nicholson TL, Olinger L, Chong K, Schoolnik G, Stephens RS. Global stage-specific gene regulation during the developmental cycle of *Chlamydia trachomatis*. J Bacteriol. 2003; 185(10):3179–89. Epub 2003/05/06. https://doi.org/10.1128/jb.185.10.3179–3189.2003 PMID: 12730178; PubMed Central PMCID: PMC154084.

38. Albrecht M, Sharma CM, Reinhardt R, Vogel J, Rudel T. Deep sequencing-based discovery of the *Chlamydia trachomatis* transcriptome. Nucleic Acids Res. 2010; 38(3):868–77. Epub 2009/11/20. https://doi.org/10.1093/nar/gkp1032 PMID: 19923228; PubMed Central PMCID: PMC2817459.

39. Humphrys MS, Creasy T, Sun Y, Shetty AC, Chibucos MC, Drabek EF, et al. Simultaneous transcriptional profiling of bacteria and their host cells. PLoS One. 2013; 8(12):e80597. Epub 2013/12/11. https://doi.org/10.1371/journal.pone.0080597 PMID: 24324615; PubMed Central PMCID: PMC3851178.

40. Grieshaber S, Grieshaber N, Yang H, Baxter B, Hackstadt T, Omsland A. Impact of Active Metabolism on *Chlamydia trachomatis* Elementary Body Transcript Profile and Infectivity. J Bacteriol. 2018;200 (14). Epub 2018/05/08. https://doi.org/10.1128/JB.00065-18 PMID: 29735758; PubMed Central PMCID: PMC6018357.

41. Rajeeve K, Vollmuth N, Janaki-Raman S, Wulff TF, Baluapuri A, Dejure FR, et al. Reprogramming of host glutamine metabolism during *Chlamydia trachomatis* infection and its key role in peptidoglycan synthesis. Nat Microbiol. 2020. Epub 2020/08/05. https://doi.org/10.1038/s41564-020-0762-5 PMID: 32747796.

42. Falkow S. Molecular Koch's postulates applied to bacterial pathogenicity—a personal recollection 15 years later. Nat Rev Microbiol. 2004; 2(1):67–72. Epub 2004/03/24. https://doi.org/10.1038/nrmicro799 PMID: 15035010.

43. Budrys NM, Gong S, Rodgers AK, Wang J, Louden C, Shain R, et al. Chlamydia trachomatis antigens recognized in women with tubal factor infertility, normal fertility, and acute infection. Obstet Gynecol.

2012; 119(5):1009–16. Epub 2012/04/25. https://doi.org/10.1097/AOG.0b013e3182519326 PMID: 22525912; PubMed Central PMCID: PMC4608258.

44. Sharma J, Zhong Y, Dong F, Piper JM, Wang G, Zhong G. Profiling of human antibody responses to Chlamydia trachomatis urogenital tract infection using microplates arrayed with 156 chlamydial fusion proteins. Infect Immun. 2006; 74(3):1490–9. Epub 2006/02/24. https://doi.org/10.1128/IAI.74.3.1490-1499.2006 PMID: 16495519; PubMed Central PMCID: PMC1418620.

45. Derré I, Pypaert M, Dautry-Varsat A, Agaisse H. RNAi screen in Drosophila cells reveals the involvement of the Tom complex in Chlamydia infection. PLoS Pathog. 2007; 3(10):1446–58. Epub 2007/10/31. https://doi.org/10.1371/journal.ppat.0030155 PMID: 17967059; PubMed Central PMCID: PMC2042019.

46. Keb G, Fields KA. Markerless Gene Deletion by Floxed Cassette Allelic Exchange Mutagenesis in Chlamydia trachomatis. J Vis Exp. 2020;(155). Epub 2020/02/18. https://doi.org/10.3791/60848 PMID: 32065159; PubMed Central PMCID: PMC7591943.

47. Stanhope R, Flora E, Bayne C, Derre I. IncV, a FFAT motif-containing Chlamydia protein, tethers the endoplasmic reticulum to the pathogen-containing vacuole. Proc Natl Acad Sci U S A. 2017; 114(45):12039–44. Epub 2017/10/29. https://doi.org/10.1073/pnas.1709060114 PMID: 29078338; PubMed Central PMCID: PMC5692559.

48. Wang Y, Kahane S, Cutcliffe LT, Skilton RJ, Lambden PR, Clarke IN. Development of a transformation system for Chlamydia trachomatis: restoration of glycogen biosynthesis by acquisition of a plasmid shuttle vector. PLoS Pathog. 2011; 7(9):e1002258. Epub 2011/10/04. https://doi.org/10.1371/journal.ppat.1002258 PMID: 21966270; PubMed Central PMCID: PMC3178582.

49. Agaisse H, Derre I. A C. trachomatis cloning vector and the generation of C. trachomatis strains expressing fluorescent proteins under the control of a C. trachomatis promoter. PLoS One. 2013; 8(2):e57090. Epub 2013/02/27. https://doi.org/10.1371/journal.pone.0057090 PMID: 23441233; PubMed Central PMCID: PMC3575495.

50. Folsch H, Pypaert M, Schu P, Mellman I. Distribution and function of AP-1 clathrin adaptor complexes in polarized epithelial cells. J Cell Biol. 2001; 152(3):595–606. Epub 2001/02/07. https://doi.org/10.1083/jcb.152.3.595 PMID: 11157985; PubMed Central PMCID: PMC2195989.